Selective laser melting of Ti6Al4V alloy for biomedical applications: temperature monitoring and microstructural evolution

I. Yadroitsev, P. Krakhmalev, I. Yadroitsava

PII: S0925-8388(13)02068-9
DOI: http://dx.doi.org/10.1016/j.jallcom.2013.08.183
Reference: JALCOM 29318

To appear in:

Received Date: 23 April 2013
Revised Date: 20 August 2013
Accepted Date: 27 August 2013

Please cite this article as: I. Yadroitsev, P. Krakhmalev, I. Yadroitsava, Selective laser melting of Ti6Al4V alloy for biomedical applications: temperature monitoring and microstructural evolution, (2013), doi: http://dx.doi.org/10.1016/j.jallcom.2013.08.183

Selective laser melting of Ti6Al4V alloy for biomedical applications: temperature monitoring and microstructural evolution

I. Yadroitsev[a,*], P. Krakhmalev[b], I. Yadroitsava[a]

[a] Université de Lyon, Ecole Nationale d'Ingénieurs de Saint-Etienne, 58 rue Jean Parot, 42023 Saint-Etienne, France

[b] Karlstad University, Department of Mechanical and Materials Engineering, SE-651 88, Karlstad, Sweden

ABSTRACT

Selective laser melting (SLM) is a kind of additive manufacturing where parts are made directly from 3D CAD data layer-by-layer from powder material. SLM products are used in various industries including aerospace, automotive, electronic, chemical, biomedical and other high-tech areas. The properties of the parts produced by SLM depend strongly on the material nature, characteristics of each single track and each single layer, as well as the strength of the connections between them. Studying the temperature distribution during SLM is important because temperature gradient and heat transfer determine the microstructure and finally mechanical properties of the SLM part. In this study a CCD camera was applied for determination of the surface temperature distribution and the molten pool size of Ti6Al4V alloy. The investigation of the microstructure evolution after different heat treatments was carried out to determine the microstructure in terms of applicability for the biomedical industry.

Keywords: titanium alloys; selective laser melting; temperature monitoring; heat treatment

[*] Corresponding author. Tel.: +33 4 77437578; fax: +33 4 7774 3497;
E-mail address: ihar.yadroitsau@enise.fr (Igor Yadroitsev)

Highlights

- Temperature measurements of molten pool were done using CCD camera
- Temperature of molten pool versus scanning speed and laser power was determined
- Microstructures and microhardness of SLM samples were analyzed
- Influence of heat treatment on microstructure were discussed and presented

1. Introduction

The remarkable ability of titanium to have two types of crystal structure – hexagonal close-packed (α-phase) and body-centered cubic structure (β-phase) – is the basis for the development of a wide range of titanium alloys with peculiar characteristics. Modification in chemical composition through alloying additions, heat treatment and processing history allows providing selected mechanical properties. Titanium alloy Ti6Al4V was developed in the early 1950s for aerospace applications and now it is known as the most commonly used titanium alloy. Ti6Al4V is α/β alloy possessing unique combination of strength, toughness and corrosion resistance, low specific weight and biocompatibility. It is used for high-performance engineering solutions in aerospace motor cases, aircraft turbines, pressure vessels and marine components [1, 2]. A range of thermo-mechanical processing of this alloy was developed and systematic studies in microstructural evolution of the Ti6Al4V alloy are carried out [3, 4]. For biomedical applications ISO 20160 “Implants for surgery” specifies the characteristics and corresponding test methods for the wrought Ti6Al4V [5].

Selective laser melting is one of “non-classical” methods to produce complex objects, under the general category of additive manufacturing [6]. To reproduce the shape of the part laser beam melts powder material layer by layer. Solidifying track by track, layer by layer, the SLM part with required geometry is created.

During selective laser melting a very small molten pool with high temperature gradients is formed. As-sintered SLM samples from Ti6Al4V have a very fine martensitic microstructure with the texture in the built direction. The microstructure of as-made SLM objects depend on material properties, process-parameters, scanning strategy and even part geometry [7–9]. Owing to specific microstructures SLM parts need to be heat treated differently than wrought alloy parts [9].

It is very important to compare the microstructure and mechanical properties of SLM parts from Ti6Al4V with the appropriate quality standards of this alloy and its products from wrought or cast material for biomedical applications. Mechanical properties of wrought and produced by laser melting Ti6Al4V alloy are close, but have a significant difference in elongation, which is higher for wrought material [10-11]. The residual stresses generated during SLM manufacturing also should be taken into account [12]. Murr et al. investigated mechanical behavior of Ti6Al4V produced by rapid-layer manufacturing and found that tensile strength was about 1.45 GPa and elongation was 4.4% [13]. Kong et al. [14] confirmed that the microstructure of the SLM Ti6Al4V alloy exhibited martenstic α' phase; ultimate tensile strength and elongation were 920-960 MPa and 3-5% correspondingly. Ramosoeu et al. [15] analysed microstructural characteristics of a direct laser sintered Ti6Al4V alloy after various heat treatments. Water quenched sample from 1100°C illustrated martensitic structure as well as higher hardness than annealed samples. Therefore to obtain the microstructures of Ti6Al4V alloy recommended for biomedical applications it is necessary to control temperature, geometrical characteristics of the molten pool during SLM process and to optimise of post heat treatment parameters.

2. Materials and methods

Ti6Al4V supplied from TLS Technik GmbH was pre-alloyed gas-atomized powder with the nominal chemical composition (wt. %): Ti – balance, Al – 5.9, V – 3.98, C – 0.006, Fe – 0.158, O – 0.160, N – 0.004, H – 0.002. Granulomorphological analysis of the particles was carried out by an optical granulomorphometer ALPAGA 500 NANO (OCCHIO s.a.). Most of the particles have high sphericity and smooth surface with some quantity of satellites (Fig. 1). The 10th, 50th and 90th percentiles of sieve diameter weighted by volume were d_{10}=8.5 μm, d_{50}=16.6 μm and d_{90}=24.7 μm, respectively. Powder had a good flowability.

Before using, the powder was dried by heating up to 80°C during 12 hours and then cooled down to room temperature in a cooling chamber. The substrate and the powder material were similar in chemical composition.

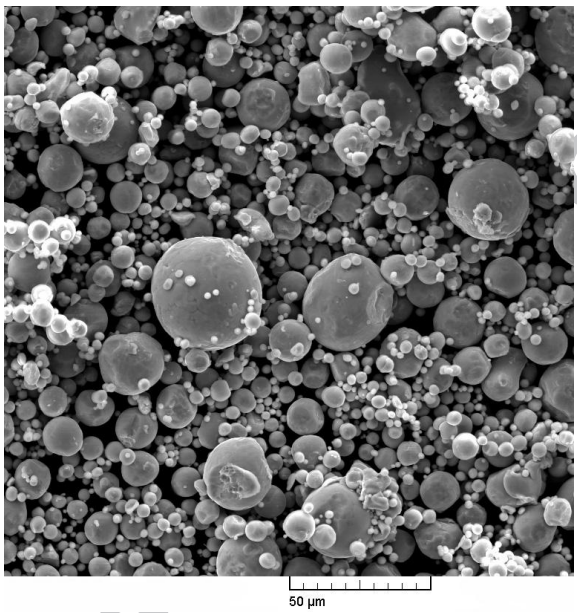

Fig. 1. SEM photo of Ti6Al4V powder.

SLM experiments were carried out using single-mode continuous-wave Ytterbium fiber laser operating at 1075 nm wavelength (IPG Photonics Corp.). The laser beam had a TEM_{00} Gaussian profile, 70 µm spot size, and 200 W maximum power. SLM samples were heat treated in a furnace at EASYLAB 304S. Argon was used as a protective atmosphere in all experiments.

Cross-sections of the samples were subjected to a standard metallographic procedure as grinding with 320, 800 and 1200 papers, and then polishing by diamond suspensions (9, 3, 1 µm size). Scanning electron microscopy (SEM) was carried out with Tescan Vega 3 at 15-20 kV accelerating voltage and 5-15 mm working distance. EDX analysis was done on Bruker EDS detector, energy spectra were calibrated to Co standard. For SEM and optical

microscope investigations cross-sections of the samples were etched in Kroll's reagent with a composition of 100 ml distilled water, 3 ml HF and 3 ml HNO_3.

To measure of the temperature distribution in the molten pool a specially designed coaxial optical system with the registration of the signal by CCD camera with the resolution 782x582 pixels was applied (Fig. 2). The signal from CCD camera was processed by a special software developed in DIPI laboratory (ENISE, France) [16].

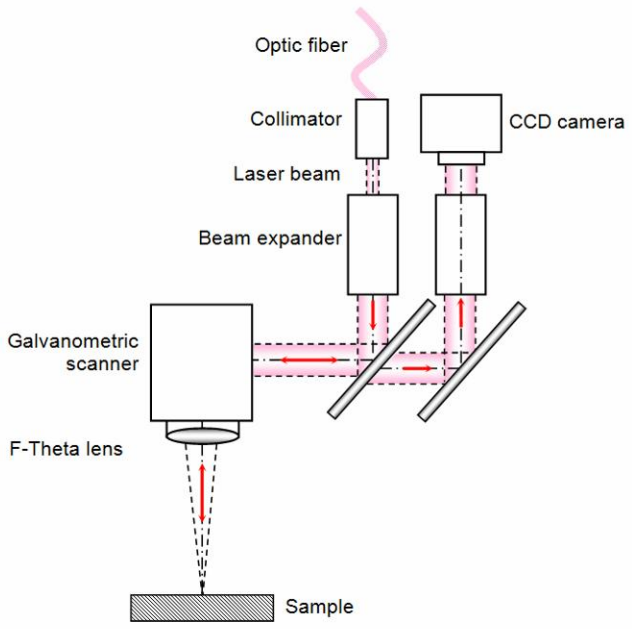

Fig. 2. Optical system for temperature measurements.

The image of the molten pool with a five time magnification was projected onto the plane of matrix-CCD-camera. The calibration of the optical system was performed by Tungsten halogen lamp as a secondary source with a transmitting diffuser diameter of 1 mm. The lamp, in turn, was calibrated by a precision blackbody source. All brightness temperatures were measured at a wavelength of 0.8 μm. For 1873 K temperature maximum error was about ±25 K.

3. Results and discussions

3.1 Geometry and temperature measurements of molten pool

At the first stage of this study the molten pool temperature at the substrate Ti6Al4V without powder was determined. The process parameters were chosen as follows: laser power (*P*) 20, 30 and 50 W, scanning speed (*V*) 0.1, 0.2 and 0.3 m/s. Series from 10 single tracks with length of 10 mm were produced on a substrate for each set of the process parameters. Typical view of a single track is shown in Fig. 3a. The molten pool and heat-affected zone (HAZ) can be clearly seen on the cross-section of track (Fig. 3b).

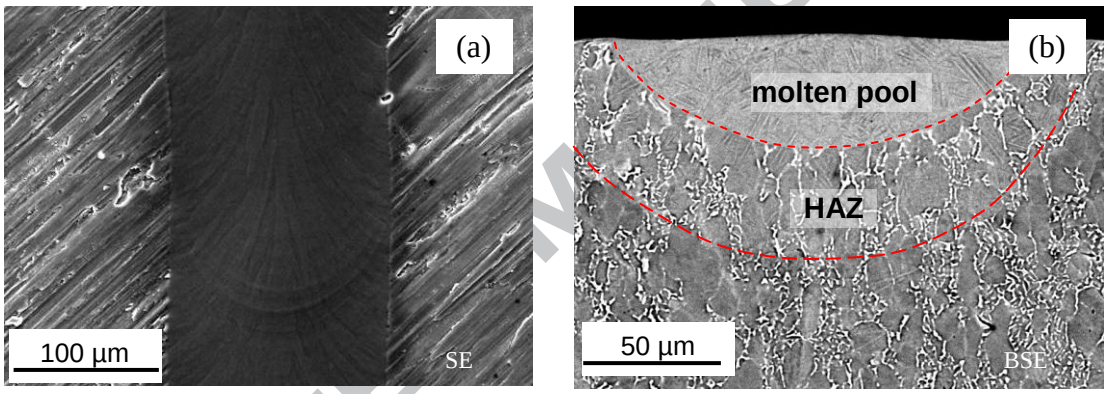

Fig. 3. SEM photos of the single track: top view (a) and cross-section (b). Laser power is 50 W, scanning speed 0.1 m/s.

The width and depth of the molten pool are increased with energy input (Fig. 4). Experimental data correlated with theoretical calculations which have been made using the Carslaw and Jaeger heat conduction equation for Gaussian heart source heat in the moving coordinate system [8, 17]. Discrepancies in the numerical values between experimental results and theoretical calculations could be associated with the complex temperature dependence of physical characteristics of irradiated material [18]. The experimental values of the width of the molten pool are notably higher than that calculated. Apparently, during laser melting of

Ti6Al4V alloy Marangoni flow plays a significant role and molten pool is shallow and wide due to emerging suface-tension-driven flows.

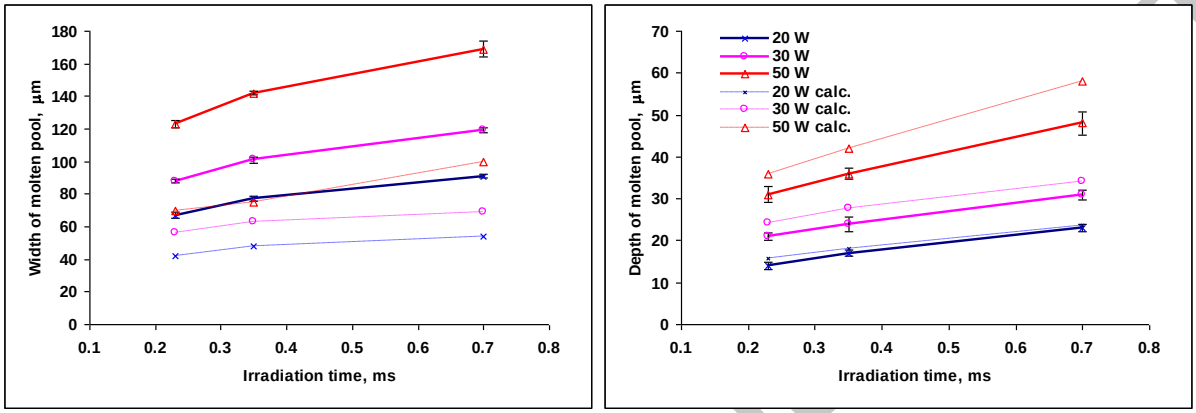

Fig. 4. The width and depth of the molten pool versus irradiation time. Irradiation time is the ratio of laser spot diameter to scanning speed.

To calculate the true temperature of the molten pool it is necessary to know the value of emissivity of the material. The emissivity is highly variable even for the same kind of material. It depends on temperature, surface texture, level of oxidation and so on. But in this study the area of solidification was registered (Fig. 5), and the solidification temperature was known value. So the emissivity was calculated using Planck's law and the true temperature of the molten pool can be calculated. The solidus temperature of Ti6Al4V about 1890 K, the brightness temperature of solidification area about 1700 K, the emissivity is $\varepsilon \sim 0.35$. Taking into account this value of emissivity and using the assumption of gray body, the maximum true temperature of the molten pool at 50 W laser power and 0.1 m/s scanning speed is about 2710 K ($T_{b,\,max}$= 2340 K). Maximum temperature of molten pool significantly increases with laser power and slightly decreases with scanning speed (Fig. 6). This is important for the selection of optimal process parameters in terms of thermal effects in SLM sample.

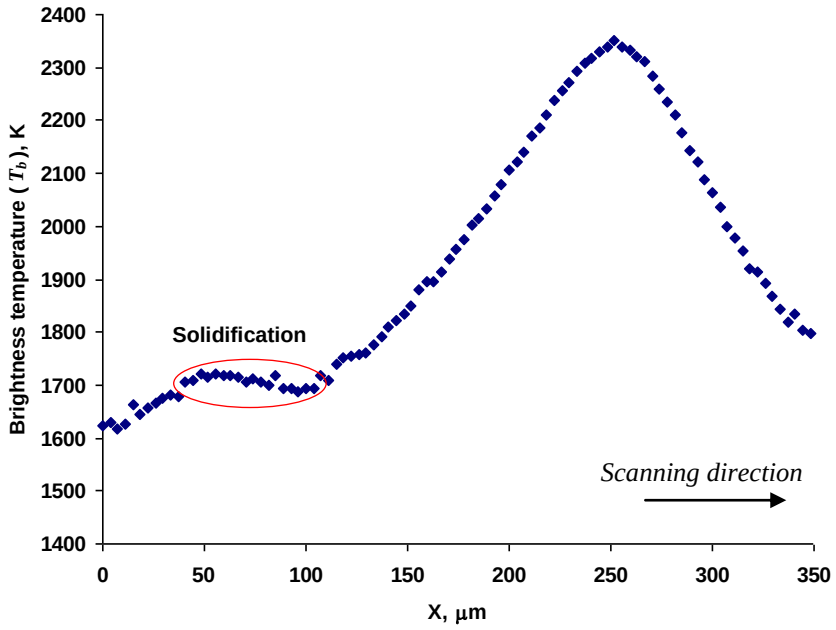

Fig. 5. Distribution of the brightness temperature in the XY-plane along the laser scanning direction; *P*=50 W, *V*=0.1 m/s.

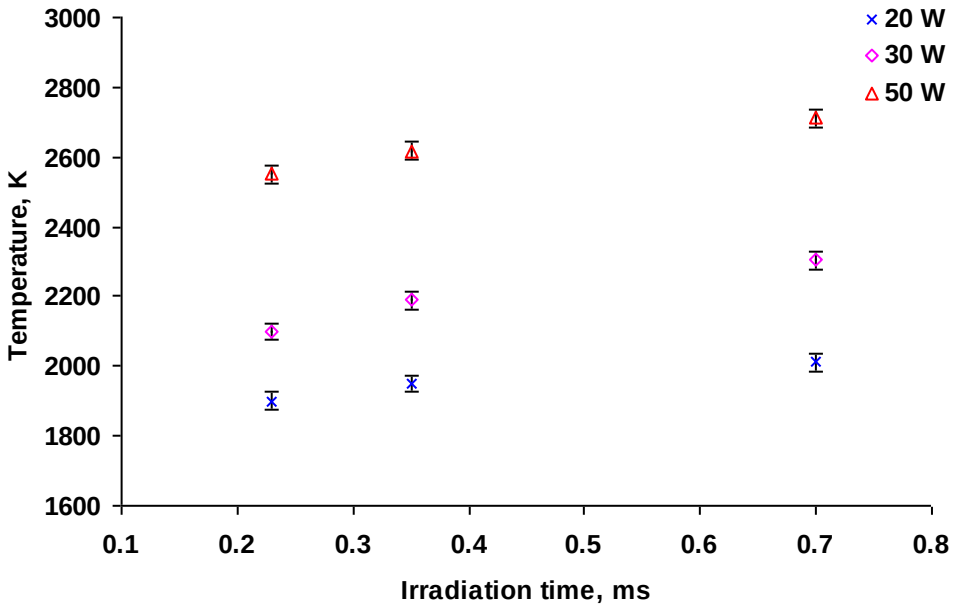

Fig. 6. The maximum true temperature of molten pool *versus* irradiation time and laser power.

High power density of the laser beam can lead to a vaporization of the irradiated material. This is especially important for laser processing of mechanical mixtures of powders with low-melting elements. The studies on evaporation behavior of alloy elements are very limited. Anand et al. [19] found that for the welding of thin samples high manganese austenitic stainless steels the composition of the weld was significantly different from the composition of the base material primarily because the loss of manganese from the weld pool. For Ti25Al25Nb alloy at 2100 K Guo et al. [20] indicated that significant loss of Al at low pressure (about 1 Pa) occurred, but with increasing the pressure (>100 Pa) in the chamber with the same temperature the evaporation loss of aluminium and the changing of chemical composition can be ignored. In this study EDX analysis in the areas of molten pool and the source material (substrate) revealed no differences in the percentage of chemical composition.

3.2 Microstructure of SLM samples

The formation of single tracks from metal powders by SLM has a threshold character: for each powder material, there exist sets of process parameters that yield stable or unstable tracks. The mechanism of distortion, irregularities and drops formation may be associated with thermophysical properties of the material, granulomorphometric characteristics of the powder, peculiarities of its deposition and spreading, layer thickness, energy parameters of laser radiation, laser scanning speed, and melt hydrodynamics [21].

It was be found that for Ti6Al4V powder layer thickness 50 μm optimal scanning speed V is 0.12 m/s and laser power P is 50 W. Two alternative scanning strategies were selected (Fig. 7a). Fist one, so-called “two-zones technique” (strategy A) [8], is applied to achieve the maximum density of the samples. Each layer of powder is processed by the laser beam twice: 1) a layer of powder is processed with a hatch distance of 120 μm; 2) a laser beam passes in between the melted tracks of the same layer thus remelting no powder but two

neighboring tracks. Another strategy was applied to minimize the number of remelting of the same area and decrease the influence of heat-affected zone (HAZ) on the final microstructure of the samples (strategy B). In the first layer a hatch distance between tracks was 120 µm. In subsequent layer the hatch distance also was 120 µm, but there was a shift of 60 µm relative to the tracks of the previous layer. Samples with dimensions of 10×10×10 mm for each of the scanning strategies were produced.

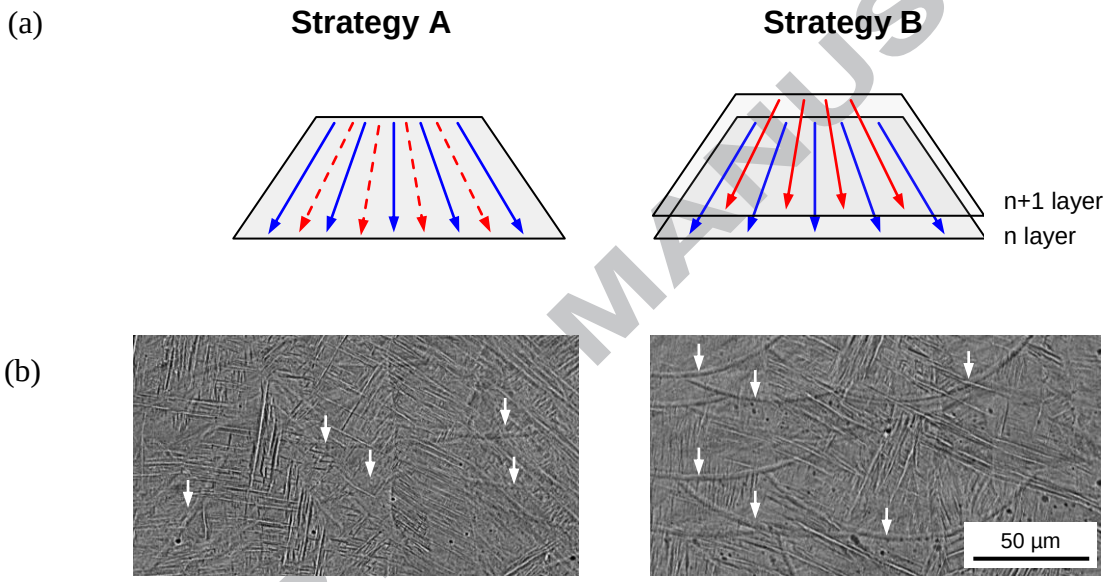

Fig. 7. Scanning strategies for SLM samples from Ti6Al4V powder (a) and SEM photos of the microstructures of specimens, white arrows indicate melt pool boundaries (b).

Microstructures of as-made samples by different SLM strategies were generally similar (Fig. 7b): the specimens had a very fine acicular morphology which could be interpreted as α' martensite [22, 23]. SLM microstructure is a result of rapid solidification and its features correlate with heat conducting direction. In Fig. 7b clearly visible melt pool

boundaries of the tracks, which may cause an anisotropy of the mechanical properties of materials [24]. More pronounced melt pool boundaries were observed for strategy B.

In accordance with the requirements for implants materials specified in the ISO 20160 [5] it is necessary to have a homogeneous equiaxial microstructure of high-density samples providing material integrity and high mechanical properties. Conventional way to control microstructure and mechanical properties of the α-β Ti alloys is selection of proper regimes of hot work and consequent heat treatment [25-27]. Heating and cooling over the β-transus temperature ($T_{\alpha-\beta}$=1000±20°C) leads to complete re-nucleation of phases. Temperature and holding time in the α+β region are heat treatment parameters controlling amount of the β-phase and the α-phase recrystallization kinetics. Transformation of the β-phase under cooling depends on the cooling rate. At the furnace and air cooling, β-phase transforms to the acicular α-Widmanstatten structure by diffusional mechanisms, water quenching (WQ) results in formation of a metastable hexagonal α'-martensite (M_s=800°C) and some residual β at grain boundaries. As seen in Fig 8a, and accordingly to other investigations [9, 22-23], cooling rate after SLM is high enough to result in formation of the α'-martensitic phase in the as-made specimen. Hardness of as-made Ti6Al4V alloy depends on process parameters [7] and generally varies between 350-500 HV, which is in a good agreement with 464±18.2$HV_{0.3}$ value observed in the present research (Fig. 9).

Acicular α+β structures, although have high fracture toughness, creep resistance and low fatigue-crack grow rate, often further heat treated to form equiaxed α-phase grains. One traditional way to form globular structure in wrought titanium alloys is annealing in the α+β region with phase recrystallization following by slow furnace cooling. This treatment is efficiently applied to α-β alloys to produce optimum combination of strength, ductility and machinability. Microstructure of the SLM Ti6Al4V alloy annealed at 800°C during 240 min following by the furnace cooling is presented in Fig 8b, it is seen that structure is still lamellar

and, there are just very few fine nuclei of the equiaxed α-phase. High stability of the lamellar structure formed by SLM has been reported for annealed Ti6Al4V alloy [9, 22, 28], only after long-term annealing at 940°C, nuclei of globular α-phase have been detected in the microstructure [9]. Mechanical strength after heat treatment of SLM alloys are usually lower compared to the as-made state [9, 28], and the coarsening of lamellar microstructure at high treatment temperatures has been suggested as the factor causing the strength decrease [9]. These results are in a good agreement with microstructural observations and hardness measurements on annealed specimen in the present research (Fig. 8b).

Another typical heat treatment aiming to increase strength characteristics of the Ti6Al4V alloy is the solute treatment at temperatures about 50°C below the β-transus (in α+β region but above M_s) following by water quenching and then tempering for several hours at 480-650°C [26]. Strengthening effect after the final treatment is achieved by precipitations in the α'-phase. Response to tempering treatment depends on amount of the α'-phase in the quenched alloy, which is controlled by the heating temperature. Generally, rise of the holding temperature causes coarsening of α-phase and increase of amount of the parental β-phase. First leads to decrease in the strength, second to increase in amount of the α'-martensite after quenching. Strengthening effect of this martensite is not high, the α'-martensite is not as hard as in ferrous alloys and causes limited hardening effect due to high dislocation density and fine lamellar structure [29], whereas coarsening of the α-phase leads to decrease in strength characteristics following the Hall-Petch relationship. As seen from the hardness measurements (Fig. 9) and observations of microstructure (Fig. 8c, e), the water quenched from 840°C alloy has finer structure and is harder compared to the one quenched from 960°C i.e. effect of coarsening dominates.

Decomposition of the hexagonal α'-martensite, accordingly to [30] accompanied with nucleation of fine α precipitates at martensite plate boundaries, enrichment of surroundings

with β-stabilizers and finally, formation of the equilibrium α+β phases mixture. At insufficiently low temperatures well below 500°C the transformation may be incomplete, but at 700-800°C will finish already after 30 min tempering [30]. Tempering of the SLM Ti6Al4V at 600°C for 4h caused 5-7% hardness increase in both specimens, water quenched from 960 and 840°C, Fig 9. Final hardness of the material quenched from 840°C and tempered, was near the value measured for the annealed specimen.

It should be noted that after all heat treatment the lines of melt pool boundaries were not observed and microstructures of the samples produced by employed SLM strategies had no differences.

It has been observed, that single nuclei of equiaxial α-phase may be found in all the materials heat-treated in the α+β region but in quite negligible contents, example for the material treated 800°C is presented in Fig 10a. Some regions of globular phase were observed in the microstructure of the material heated up to 960°C. Those regions, enriched by alpha-stabilizing Al, have rather equiaxed morphology but formed locally and unevenly distributed in microstructure, Fig. 10b.

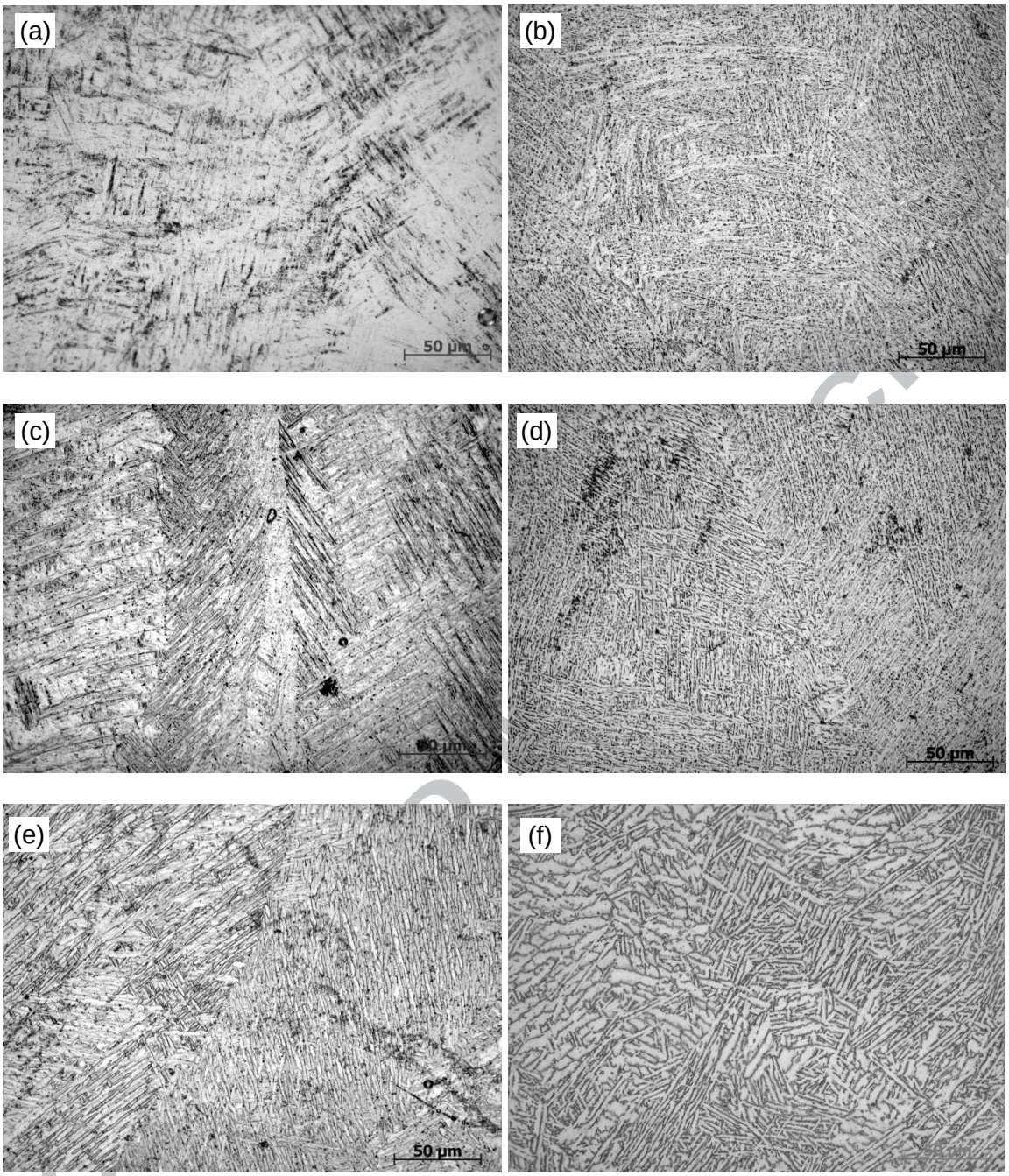

Fig. 8. Microstructure of Ti6Al4V: (a) after SLM process; (b) annealing 4h at 800°C; (c) WQ/840°C; (d) WQ/840°C + tempering/600°C/4 hr; (e) WQ/960°C; (f) WQ/960°C + tempering/600°C/4 hr.

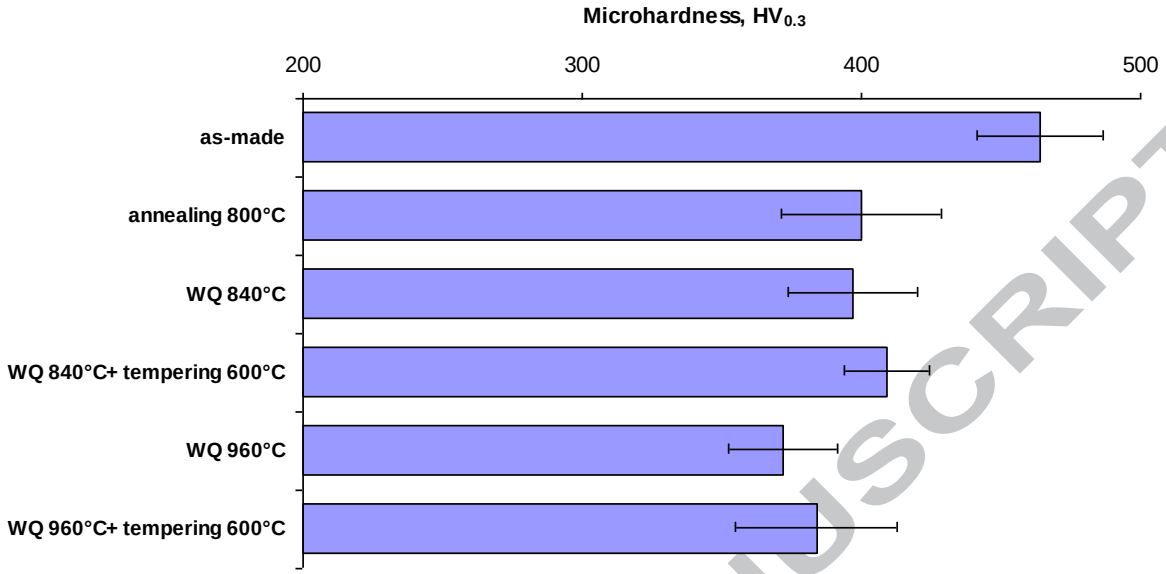

Fig. 9. Vickers microhardness of Ti6Al4V alloy.

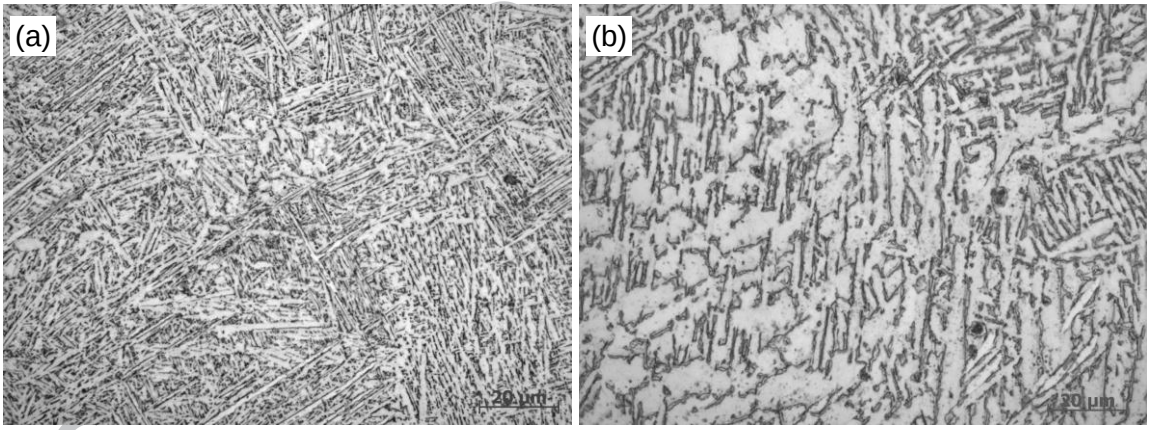

Fig. 10. Nuclei of equiaxial α-phase in Ti6Al4V annealed 4h at 800°C (a); at WQ/960°C + tempered 600°C/4 hr (b).

4. Conclusion

The on-line optical monitoring system with CCD camera was employed for the measurement of brightness temperature in the laser irradiation zone. Solidification temperature was used as reference point to calculate maximal true temperature of molten

pool. The results indicate that the maximum temperature of molten pool increased significantly with laser power and slightly increased with irradiation time. The width and depth of the molten pool behaviour correlated well to temperature changing *versus* scanning parameters. This is important for the selection of optimal process parameters in terms of thermal effects in SLM process.

Post-heat treatment of as-made SLM samples caused phase transformation and some microstructural changes but did not resulted in formation of the microstructure recommended for surgery implants in ISO 20160 standard. The texture in the form of melt pool boundaries was not observed and the microstructure still was fine. Nevertheless, some regions of globular phase were observed in the microstructure of the material heated up to 960°C, which implies that increase of holding time or temperature can lead to formation of significant fractions of globular alpha phase uniformly distributed in microstructure.

References

[1] International Titanium Association, www.titanium.org.

[2] M.A. Imam, A.C. Fraker, Titanium alloys as implant materials, in: S.A. Brown, J.E. Lemons (Eds.), Medical applications of titanium and its alloys, ASTM Special Technical Publication, 1996, pp. 3–16.

[3] R. Ding, Z.X. Guo, A. Wilson, Microstructural evolution of a Ti–6Al–4V alloy during thermomechanical processing, Mater. Sci. Eng. A 327 (2002) 233–245.

[4] R. Filip, K. Kubiak, W. Ziaja, J. Sieniawski, The effect of microstructure on the mechanical properties of two-phase titanium alloys, J. Mater. Process. Technol. 133 (2003) 84–89.

[5] ISO 20160:2006: Implants for surgery – Metallic materials – Classification of microstructures for alpha+beta titanium alloy bars.

[6] T. Wohlers, Wohlers Report 2010: Additive manufacturing state of the industry. Annual world wide progress report, Wohlers Associates, Fort Collins, 2010.

[7] L. Thijs, F. Verhaeghe, T. Craeghs, J. Van Humbeeck, J.-P. Kruth, A study of the microstructural evolution during selective laser melting of Ti–6Al–4V, Acta Mater. 58 (2010) 3303–3312.

[8] I. Yadroitsev, Selective laser melting: Direct manufacturing of 3D-objects by selective laser melting of metal powders, LAP Lambert Academic Publishing AG & Co KG, 2009.

[9] B. Vrancken, L. Thijs, J. P. Kruth, J. Van Humbeeck, Heat treatment of Ti6Al4V produced by selective laser melting: microstructure and mechanical properties, J. Alloy Compd. 541 (2012) 177–185.

[10] ASTM F136 - 12a Standard specification for wrought titanium-6aluminum-4vanadium ELI (extra low interstitial) alloy for surgical implant applications (UNS R56401).

[11] ASTM F2924 - 12a Standard specification for additive manufacturing titanium-6aluminum-4vanadium with powder bed fusion.

[12] M. F. Zaeh, G. Branner, Investigations on residual stresses and deformations in selective laser melting, Prod. Eng. 4 (2010) 35–45.

[13] L.E. Murr, S.A. Quinones, S.M. Gaytan, M.I. Lopez, A. Rodela, E.Y. Martinez, D.H. Hernandez, E. Martinez, F. Medina, R.B. Wicker, Microstructure and mechanical behavior of Ti–6Al–4V produced by rapid-layer manufacturing, for biomedical applications, J. Mech. Behav. Biomed. 2 (2009) 20–32.

[14] C.J. Kong, C.J. Tuck, I. A. Ashcroft, R.D. Wildman, R. Hague, High density Ti6Al4V via SLM processing: microstructure and mechanical properties, in: Proc. of Solid Freeform Fabrication Symposium, Austin, Texas, USA, 2011, pp. 475-483.

[15] M.E. Ramosoeu, H.K. Chikwanda, A.S. Bolokang, G. Booysen, T.N. Ngonda, Additive manufacturing: characterization of TI-6AI-4V alloy intended for biomedical application, in: Proc. of Light Metals Conference, The Southern African Institute of Mining and Metallurgy Advanced Metals Initiative, 2010, pp. 337-344.

[16] Yu. Chivel, I. Smurov, Temperature monitoring and overhang layers problem, Phys. Procedia 12 (2011) 691–696.

[17] A.V. Gusarov, I. Yadroitsev, Ph. Bertrand, I. Smurov, Model of radiation and heat transfer in laser-powder interaction zone at selective laser melting, ASME J. Heat Transfer. 131 (2009) 072101-072109.

[18] S. Kou, Welding metallurgy, second ed., Wiley–Interscience, New Jersey, 2003.

[19] J.P. Anand, A.A. Khan, Analysis of mass transport during laser welding, in: Proc. of SPIE Int. Soc. Opt. Eng., Society of Photo-Optical Instrumentation Engineers: Bellingham, WA, USA, 1990, pp. 198-207.

[20] J.J. Guo, G.Z. Liu, Y.Q. Su, H.S. Ding, J. Jia, H.Z. Fu, Evaporation of multi-components in Ti-25Al-25Nb melt during induction skull melting process, Trans. Nonferrous. Met. Soc. China. 12 (2002) 588-591.

[21] I. Yadroitsev, A. Gusarov, I. Yadroitsava, I. Smurov, Single track formation in selective laser melting of metal powders, J. Mater. Process. Technol. 210 (2010) 1624-1631.

[22] L. Facchini, E. Magalini, P. Robotti, A. Molinari, S. Hoges, K. Wissenbach, Ductility of a Ti-6Al-4V alloy produced by selective laser melting of prealloyed powders, Rapid Prototyping J. 16 (2010) 450–459.

[23] M. Simonelli, Y.Y. Tse, C. Tuck, Microstructure of Ti-6Al-4V produced by selective laser melting, JPCS (IOP Publishing) 371 (2012) 012084.

[24] I. Yadroitsev, L. Thivillon, Ph. Bertrand, I. Smurov, Strategy of manufacturing components with designed internal structure by selective laser melting of metallic powder, Appl. Surf. Sci. 254 (2007) 980-983.

[25] C. Leyens, M. Peters, Titanium and titanium alloys: fundamentals and applications, Wiley-VCH Verlag GmbH & Co, 2003.

[26] M.J. Donachie Jr. Titanium: a technical guide, 2nd ed.: ASM International, Materials Park, 2000.

[27] R. Boyer, E.W. Collings, G. Welsch (eds.), Materials properties handbook: titanium alloys, ASM International, 1994.

[28] M. Thöne, S. Leuders, A. Riemer, T. Tröster, H.A. Richard, Influence of heat-treatment on selective laser melting products – e.g. Ti6Al4V, in: Solid Freeform Fabrication symposium, Austin, Texas, USA, 2012.

[29] A. Russell, K.L. Lee, Structure-property relations in non-ferrous metals, John Wiley and Sons, Hoboken, NJ, 2005.

[30] F.X. Gil Mur, D. Rodriguez, J.A. Planell, Influence of tempering temperature and time on the α'-Ti-6Al-4V martensite, J. Alloy. Compd. 234 (1996) 287-289.

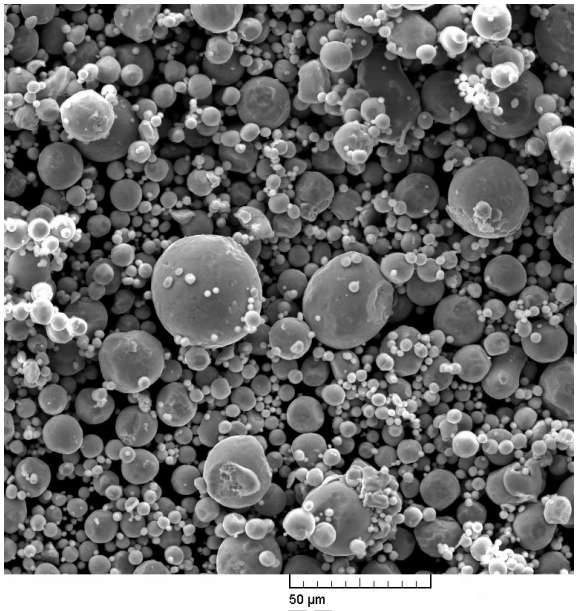

Fig. 1. SEM photo of Ti6Al4V powder.

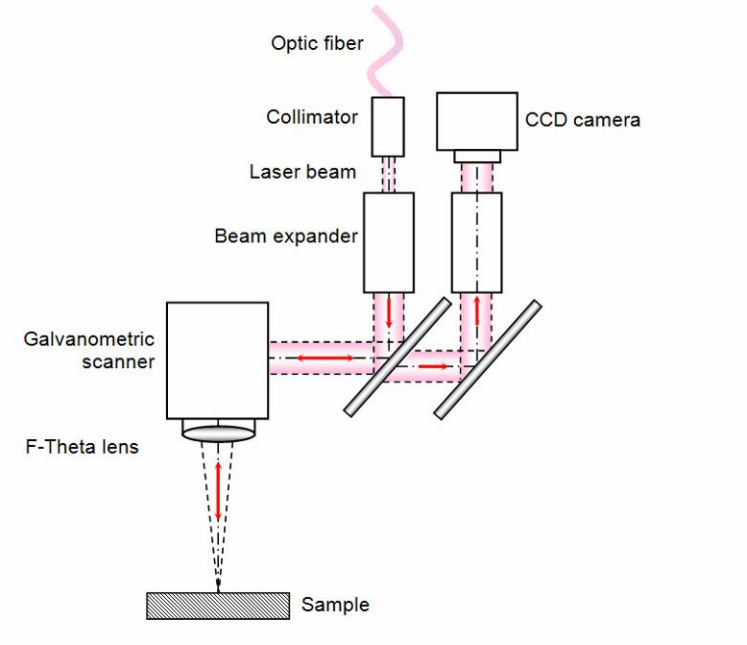

Fig. 2. Optical system for temperature measurements.

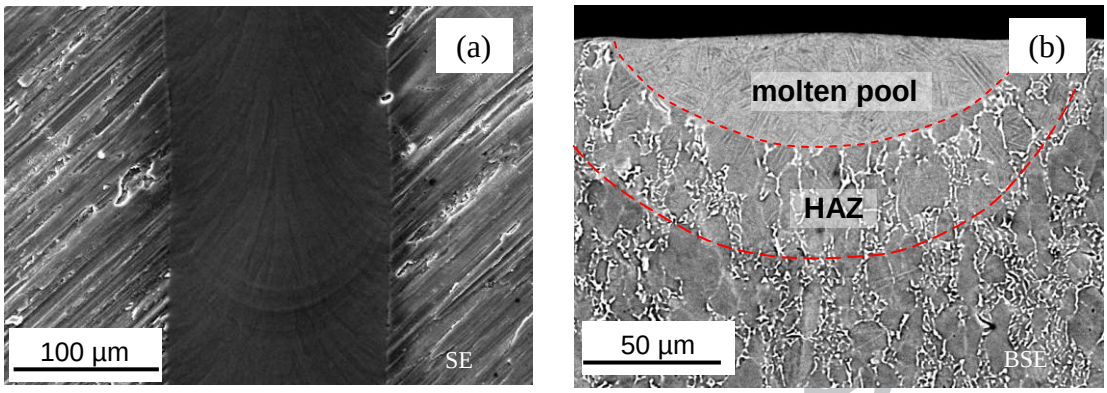

Fig. 3. SEM photos of the single track: top view (a) and cross-section (b). Laser power is 50 W, scanning speed 0.1 m/s.

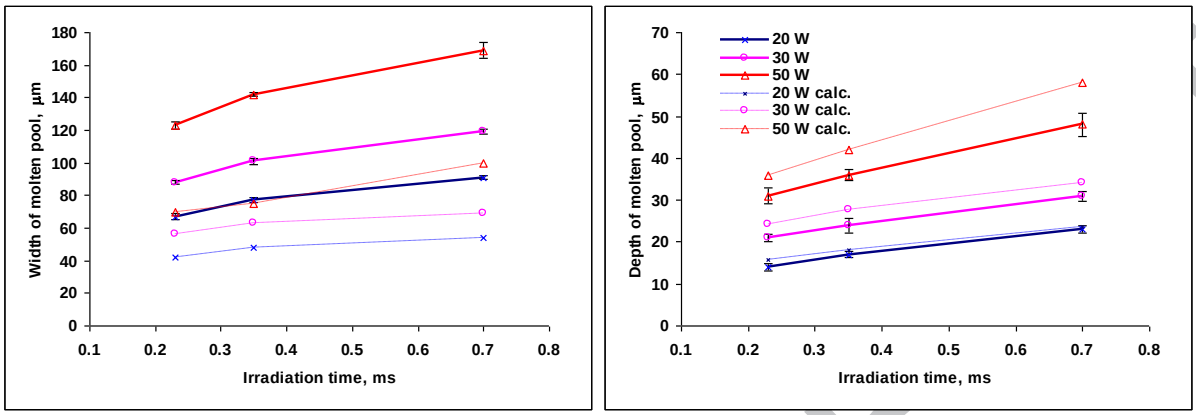

Fig. 4. The width and depth of the molten pool versus irradiation time. Irradiation time is the ratio of laser spot diameter to scanning speed.

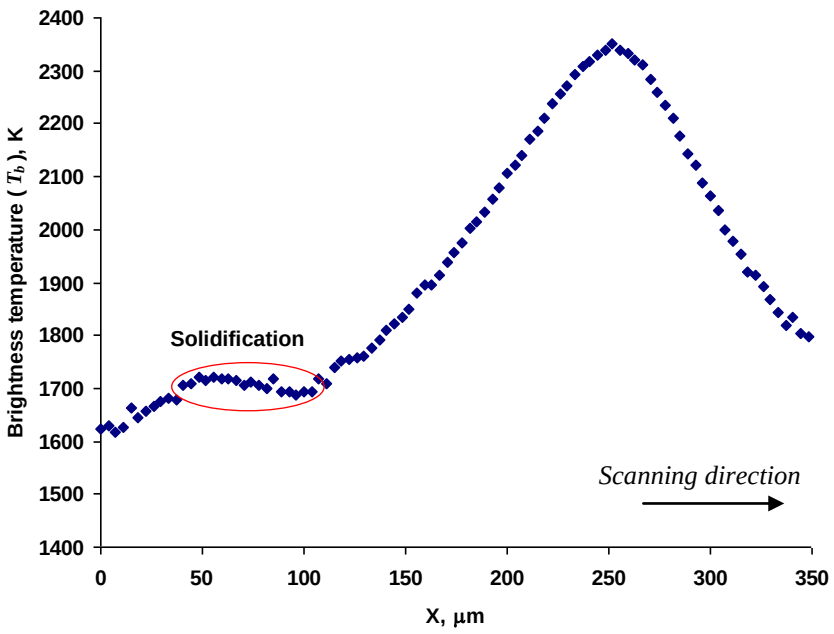

Fig. 5. Distribution of the brightness temperature in the XY-plane along the laser scanning direction; *P*=50 W, *V*=0.1 m/s.

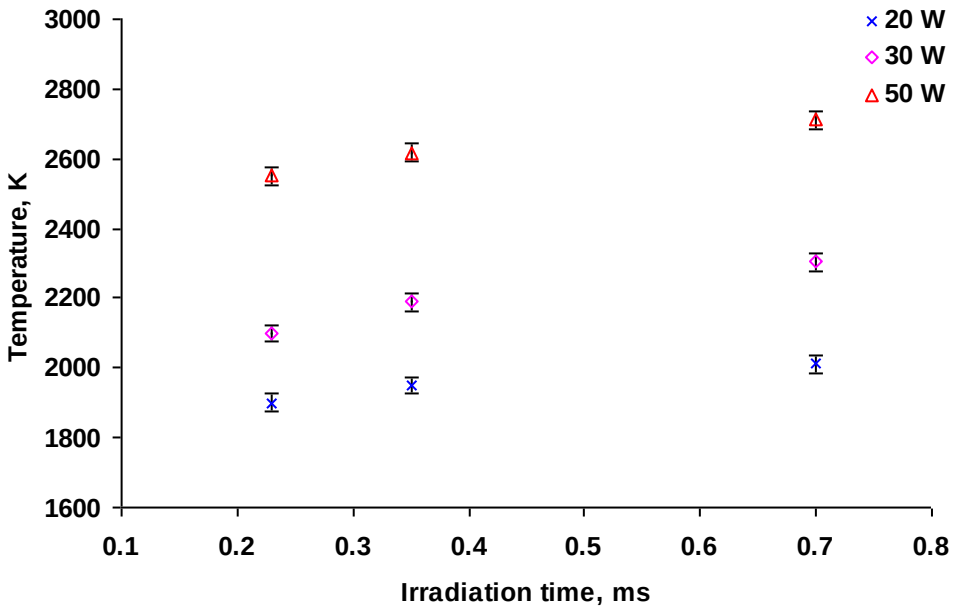

Fig. 6. The maximum true temperature of molten pool *versus* irradiation time and laser power.

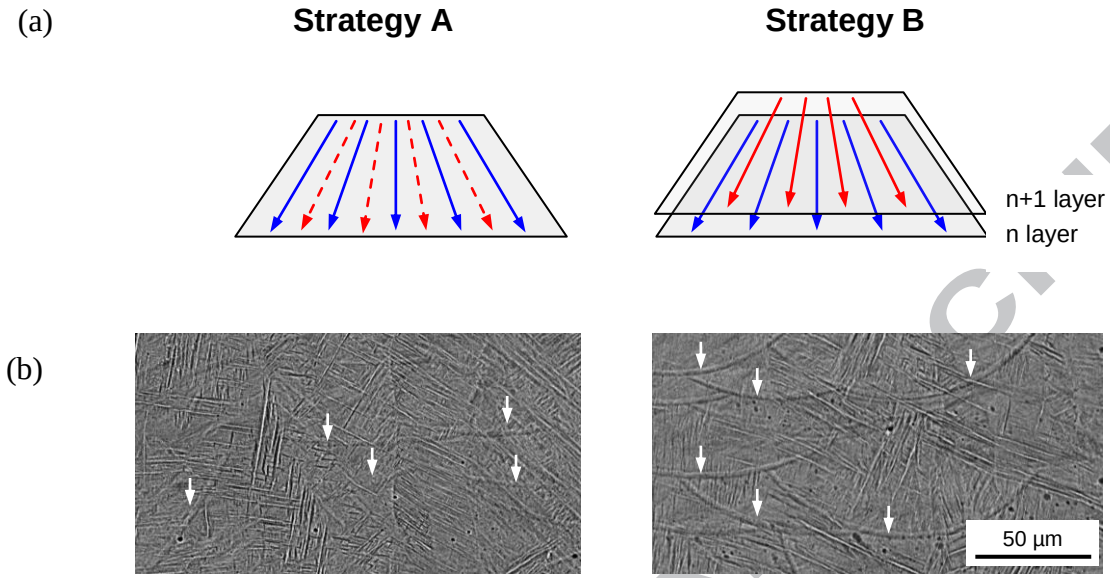

Fig. 7. Scanning strategies for SLM samples from Ti6Al4V powder (a) and SEM photos of the microstructures of specimens, white arrows indicate melt pool boundaries (b).

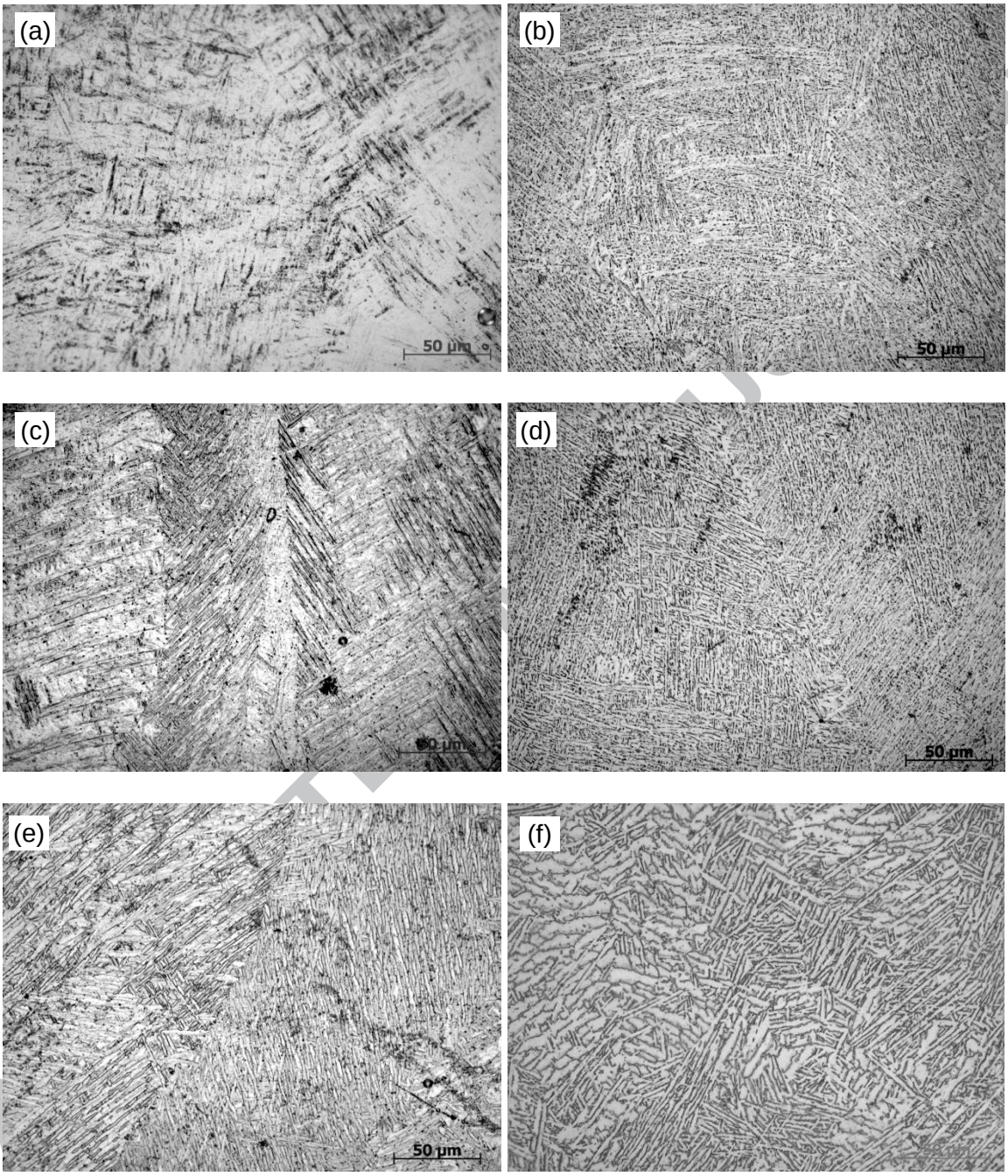

Fig. 8. Microstructure of Ti6Al4V: (a) after SLM process; (b) annealing 4h at 800°C; (c) WQ/840°C; (d) WQ/840°C + tempering/600°C/4 hr; (e) WQ/960°C; (f) WQ/960°C + tempering/600°C/4 hr.

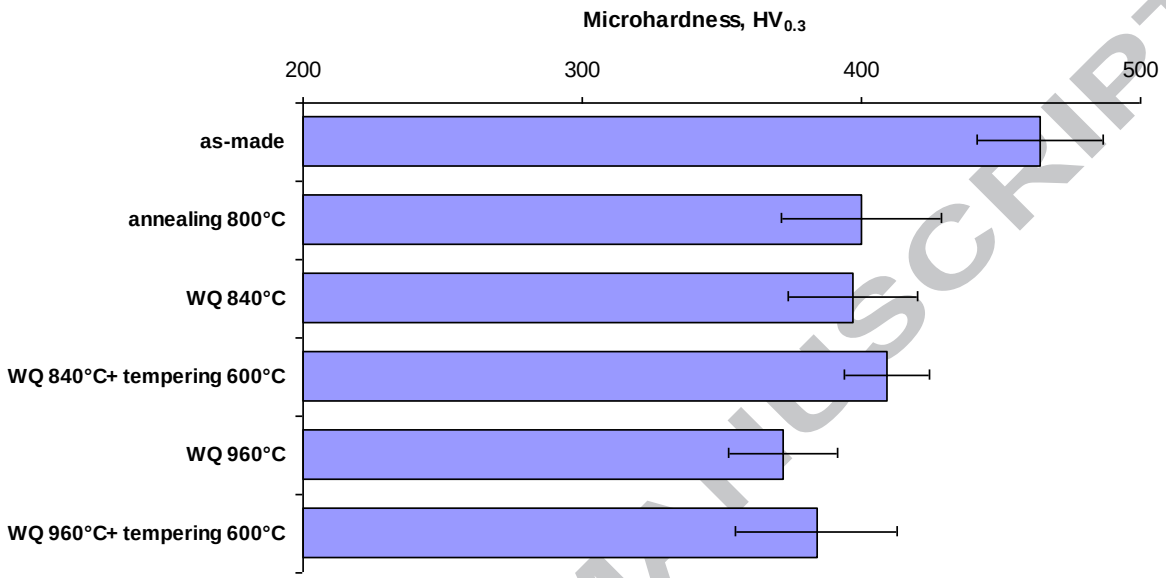

Fig. 9. Vickers microhardness of Ti6Al4V alloy.

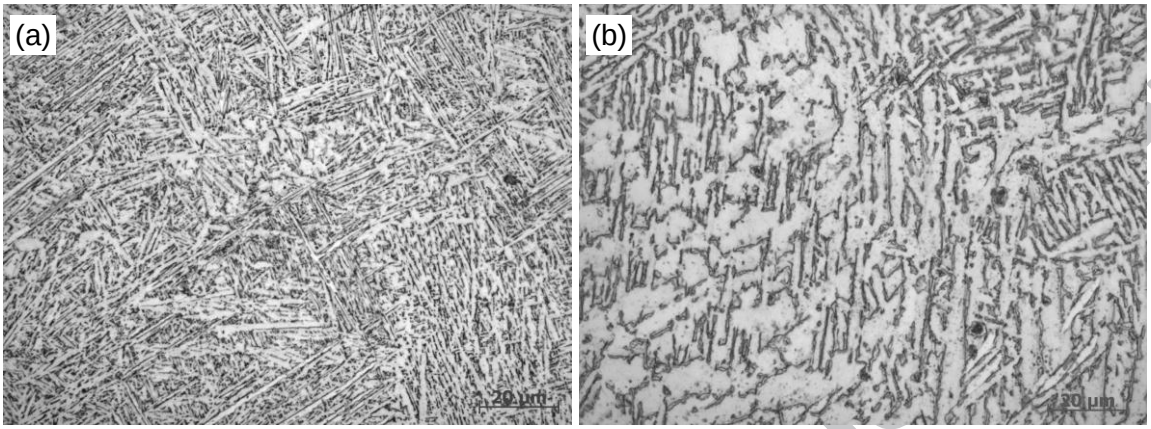

Fig. 10. Nuclei of equiaxial α-phase in Ti6Al4V annealed 4h at 800°C (a); at WQ/960°C + tempered 600°C/4 hr (b).

Highlights

- Temperature measurements of molten pool were done using CCD camera
- Temperature of molten pool versus scanning speed and laser power was determined
- Microstructures and microhardness of SLM samples were analyzed
- Influence of heat treatment on microstructure were discussed and presented